METHODS FOR IMPROVING SEISMIC EVENT LOCATION PROCESSING

Clifford H. Thurber and Haijiang Zhang

University of Wisconsin-Madison

Sponsored by Air Force Research Laboratory

Contract No. DTRA01-01-C-0085

ABSTRACT

Our research program consists of four components, each involving some aspect of multiple-event analysis: (1) high-precision waveform cross-correlation (WCC) for arrival time estimation, (2) robust event clustering, (3) waveform decomposition and source wavelet deconvolution reshaping, and (4) double-difference (DD) multiple-event location and tomography. Our research focused initially on the development and testing of these seismic analysis methods using "ground-truth" (GT) datasets at different scales (local and regional), and was followed by the application of these methods to real-time and simulated real-time data streams. Here we summarize the more significant project achievements in the four research areas.

(1) Differential arrival times for pairs of seismic events observed at the same station are often calculated by WCC. Researchers often choose the differential times to use based on the associated cross-correlation (CC) values exceeding a specified threshold. When two similar time series are contaminated by significant noise, or in the case of cycle skipping, the time delay calculated with the WCC technique may not be reliable even if it exceeds the specified threshold. If the threshold is set too high, then only a limited number of very precise differential time data are available to constrain the relative positions of earthquakes. If the threshold is set too low, then many unreliable differential time estimates are used and they will negatively affect the relocation results. The bispectrum method can suppress the Gaussian or low-skewness noise sources in two similar time series and can be used to obtain a second, independent estimate of the relative time delay between them. We compute time delay estimates between the waveform pairs with the bispectrum method and use them to verify the WCC-determined one. This technique can provide quality control for the time delay estimates, and can potentially provide more differential time data for close event pairs by verifying the reliability of differential times that might not meet the threshold criterion.

(2) We have tested a two-step clustering and location technique with a California GT dataset. In Step 1, event locations are estimated via WCC of Hilbert-envelope waveforms. The Step 1 procedure located the epicenters within 20 km (approximately 1 bin) of the catalog location for 16 of the 20 test events. However, depth estimates were poorly constrained. The Step 2 refinement based on WCC of the high-frequency P arrivals followed by DD relocation improved both epicenter and depth estimates. This two-step procedure offers advantages over conventional location techniques including a Step 1 event clustering and preliminary location not dependent on the accuracy of catalog picks and a Step 2 improvement using the high-precision DD technique.

(3) We tested a variety of decomposition and filtering techniques with the multiple goals of noise reduction, waveform "homogenization" (reshaping to similar "wavelet"), and depth phase identification. Methods examined include eigenimage decomposition, KLD, CANC, and coherency filtering. A key issue is the effect of arrival misalignment between a pair of traces on the success of a given technique. We tested a two-stage process whereby the similarity and strength of a CANC-filtered trace (relative to the original and error traces, respectively) is used to align the trace to the reference signal. We also developed a wavelet-based auto-picker for detecting and picking first-P arrivals that can be used in conjunction with our location processing procedures, both for identifying waveform segments for correlation and for adjusting stack picks.

(4) We have developed the new method of DD tomography. The code tomoDD takes the DD location method (hypoDD) a step further to solve for three-dimensional (3D) velocity structure simultaneously with hypocenter locations, using both catalog picks and differential arrival times. Compared to conventional tomography, the result is a sharpening of the seismicity distribution equal in quality to hypoDD plus a sharpening of the velocity image due to removal of the majority of the location scatter. We have developed local- and regional-scale versions of tomoDD, and have applied each to synthetic and real datasets. We have also developed a version of the new location code locOO.

OBJECTIVES

Our research program consists of four components, each involving some aspect of multiple-event analysis: (1) high-precision WCC for arrival time estimation, (2) robust event clustering, (3) waveform decomposition and source wavelet deconvolution reshaping, and (4) DD multiple-event location and tomography. Our research focused initially on the development and testing of these seismic analysis methods using GT datasets at different scales (local and regional), and was followed by the application of these methods to real-time and simulated real-time data streams.

RESEARCH ACCOMPLISHED

High-precision waveform cross-correlation for arrival time estimation

When two earthquakes have close hypocenters and share similar source mechanisms, they will generate similar ground motions. It is possible to obtain very accurate differential times from waveform data for such nearby events, and use them to improve location results (e.g., Shearer, 1997; Rubin *et al*., 1999; Waldhauser and Ellsworth, 2000; Schaff *et al*., 2002, Rowe *et al*., 2002), or combine them with absolute arrival times to invert for high-quality 3D velocity structure (Zhang and Thurber, 2003). Such studies generally use a WCC technique to calculate the relative time delay between the waveforms of two events recorded at the same station. For very similar traces, some researchers obtain a time delay to the sub-sample level by a weighted linear fitting of the cross spectral phase after first aligning the two waveforms with the cross-correlation- (CC-) determined lag (Poupinet *et al*., 1984). The calculated time delay has an associated CC coefficient whose value may not be very high if the underlying signals are not time-delayed similar waveforms, or if the underlying time-delayed signals are contaminated by high levels of noise. It is hard to differentiate these two possible causes, especially when many thousands or more waveforms are being analyzed automatically. Thus researchers often choose those time delay estimates with CC coefficients above a specified threshold. For example, Schaff *et al*. (2002) only select those time delays with CC values larger than 0.70 and mean coherences above 0.70.

The selection of an optimum threshold value is important but difficult. If it is set too high, then only a limited number of very accurate differential time data are available to constrain the relative positions of earthquakes. If the threshold value is set too low, then many unreliable differential time estimates, which are used, can negatively affect the relocation results. Du *et al.* (2004) deal with this problem by computing additional estimates of the time delay with the bispectrum (BS) method. The BS method, which works in the third-order spectral domain, can suppress correlated Gaussian or low-skewness noise sources (Nikias and Raghuveer, 1987; Nikias and Pan, 1988). Du *et al.* (2004) adopt this method to calculate two additional time delay estimates with both the raw (unfiltered) and band-pass filtered waveforms, and use them to verify (select or reject) the one computed with the CC technique using the filtered waveforms. This BS verification process can reject unreliable CC time delay estimates and also can accept additional CC time delays even if their associated CC coefficients are smaller than some threshold value, if they pass the BS checking procedure. We do not claim that the BS method always obtains a better time delay estimate than the CC technique, but use it to check the reliability of the time delay estimates computed with the CC technique. By applying two different methods that work in different spectral domains (second- and third-order), we can improve the reliability of the selected time delays. The two BS time delay estimates do not always agree with each other because the characteristics of noise in the raw and filtered waveforms are different. Therefore checking the values of the CC time delay against both of them provides additional quality control.

Figure 1 shows examples of the application of the BS verification method to waveforms recorded at New Zealand stations for two pairs of relatively close events. In Figure 1a, the CC value (0.74) is above the nominal threshold (0.70), but the lag does not agree with that obtained from the bispectrum (bottom panel), so this CC value is rejected. From the seismograms, we can see that this is apparently a case of cycle skipping - the filtered waveforms coincidentally correlate slightly better at a lag of -10. In Figure 1b, both methods provide the same time delay, but the associated CC coefficient is only 0.50. Under the threshold criterion, such a time delay estimate associated with a low CC coefficient is simply discarded. Using the BS checking method we can identify the reliable time delays from these "seemingly not very similar" waveforms, such as for this pair, and as a result provide more control over the relative locations of the events. Du *et al.* (2004) apply this technique to 822 New Zealand earthquakes in the Wellington area and find that the CC time delays verified with the BS method provide improved earthquake relocation results (noticeably more clustered) compared to those selected with the standard threshold criterion. An example of the improvement of the BS-verified locations compared to original catalog locations, DD locations using differential catalog picks, and DD locations using standard threshold CC lags is shown in Figure 2 for a sub-region near Lake Wairarapa.

Robust event clustering

An adaptive, automatic phase-picking and epicenter-location program is now fully developed and is being applied to update the New Mexico microseismicity catalog. The program is built upon the MATLAB environment using MatSeis (Young, *et al.*, 2002). The package is named PLRR (Pick-Locate-Repick-Relocate). The key strategy of PLRR is to find the event from a reference database that is most similar to a new event according to the spectrogram cross-correlation, and to use the alignment with the similar reference event to assign phase picks to the new event. No preliminary pick or location information is needed for the new event.

The following are some key characteristics of the PLRR package.

(1) Data format: the seismic data format recognized by PLRR is the CSS-3.0 flatfile format.

(2) Reference database: the quality of phase-picking and epicenter-location results will ultimately depend on the coverage and quality of the reference database (Figure 3).

(3) Spectrogram cross-correlation: we find for this data set that the spectrogram is most diagnostic and discriminates events best within a limited bandwidth between 6 and 10 Hz.

(4) Waveform-pair match and event-pair match: we have explored two options in PLRR to find phases and locations for unknown events. The first, waveform-pair matching, finds the most similar waveforms in the reference database, station by station, and after alignment, assigns the corresponding phase information to the new waveforms. This technique was found to produce too many false associations. The second, event-pair matching, is more robust. This option stacks the cross-correlation coefficient curves of waveform-pairs between the new event and waveforms grouped from each event in the reference database, and finds the reference event that has the highest stacked CC coefficient value (by taking the mean/median of stacked CC coefficient curves).

(5) Database operation: several simple functions to enhance and simplify the operation of CSS-3.0 database are added into PLRR, such as the "Update monthly table," which adds a new event to a CSS-3.0 database.

PLRR was developed to process the seismic data of New Mexico, and we have not tested our code on other seismic networks Users from other areas will have to modify the PLRR code to apply it to their situation, including building travel-time tables and modifying *site* and *sitechan* tables. PLRR also defaults to a sample rate of 100 samples per second. For the New Mexico region, we use PLRR to process the seismic data generated by an Earthworm data acquisition system on a month-by-month basis. Visual checking is applied to ensure that the automatic results are valid and that events arising from new source regions are properly added to the reference database. Given enough representative seismicity, the system should progressively increase in its accuracy.

A two-step clustering and location version of PLRR was also tested with a California GT data set. In step 1the event locations are estimated using WCC of Hilbert-envelope waveforms. This procedure located the epicenters within 20 km of the catalog location for 16 of the 20 test events; however, the depth estimates were poorly constrained. The Step 2 refinement, based on WCC of the high-frequency P arrivals followed by DD relocation improved both epicenter and depth estimates. This two-step procedure offers advantages over conventional location techniques including event clustering and preliminary location not dependent on the accuracy of catalog picks and subsequent location improvement using the high-precision DD technique.

Waveform decomposition and source wavelet deconvolution reshaping

We tested a variety of decomposition and filtering techniques with the multiple goals of noise reduction, waveform "homogenization" (reshaping to similar "wavelet"), and depth phase identification. The methods examined include eigenimage decomposition, KLD, Correlated data Adaptive Noise Canceling (CANC), and coherency filtering. A key issue is the effect of arrival misalignment between a pair of traces on the success of a given technique. Some methods rely on signals being time-aligned before processing, which of course cannot be assumed for seismic data in a monitoring context. We also developed a wavelet-based auto-picker for detecting and picking first-P arrivals that can be used in conjunction with our location processing procedures, both for identifying waveform segments for correlation and for adjusting stack picks (Zhang *et al*., 2003b).

A recent paper by Ulrych *et al*. (1999) reviews several decomposition and transformation techniques that are useful for signal-noise separation in an exploration seismic context. The two most relevant to our work are eigenimage

decomposition and Karhunen-Loéve decomposition (KLD). KLD is distinguished from the more common eigenimage decomposition (essentially principal components) in that the latter extracts eigenvector-eigenvalue information from multi-channel data based on a covariance matrix computed at a single lag (zero), whereas the former carries out a decomposition for single-channel data based on a covariance matrix for multiple lags (Ulrych *et al*., 1999). In practice, to apply KLD to multi-channel data, an average covariance matrix can be computed.

The utility of the KLD method for extracting similar signals from noisy data is being tested. A synthetic example is shown in Figure 4. In this particular case, we construct initially noise-free seismograms (upper left panel) that consist of a first-arriving signal that is time-aligned and an identical second-arriving signal with substantial moveout. Gaussian noise with root mean square (RMS) amplitude, 20% of the signal amplitude, is added (upper right panel) and eigenimage decomposition (not shown) and KLD (Figure 4) are carried. The eigenimage decomposition, using eigenvalues of average value and greater, preserves the time-aligned signal but degrades the secondary arrival, leaving most of the latter's energy in the residual "noise." KLD (middle left panel), again using eigenvalues of average value and greater (bottom left panel), preserves both the time-aligned signal and the secondary arrival (middle right panel).

For a second example, we apply KLD to real data from a group of earthquakes of magnitude 3.6 to 3.8 in Long Valley, California from January 1998. In the catalog, the events are within about 1 km of each other in epicenter but have estimated depths ranging from 0.5 to 5.0 km. Relocation using hypoDD and catalog arrival times plus catalog-generated arrival time differences yields epicenters within less than 1 km and depths within 250 m of each other. The analyzed waveforms were recorded at station ORV with an epicentral distance of 314 km.

The results of the KLD analysis are shown in Figure 5. The raw data traces are relatively noisy. In this case, we recognize that the eigenvectors for the four largest eigenvalues represent long-period noise (bottom left panel), and we exclude them along with the smaller eigenvalues. The resulting KLD-processed traces (upper right panel) are quite similar and the data residue (middle left panel) contains no obvious remnant signal of interest. In contrast, the eigenimage decomposition does little if anything to improve the signal similarity, only removing some of the higher frequency noise.

An alternative approach to noise reduction by extracting common waveform signals is adaptive filtering. We have experimented with a CANC algorithm of Hattingh (1988). Input into the CANC procedure consists of a "reference signal" S1 and a "primary signal" S2, correlated to each other in some unknown way. Each signal is presumed to contain noise that is uncorrelated with the noise from the other trace. The reference signal is used as a "learning signal" to derive filter coefficients. The filter adjusts its impulse response to minimize the mean-squared error between filter output and the primary signal (in terms of power). The algorithm rapidly solves for the filter coefficients without requiring matrix inversion or a CC operation. The CANC procedure is an iterative solution, computing updated filter coefficients at each iteration.

The CANC procedure is applied to seismic data from two events in a cluster with similar catalog epicenters but different depths, recorded at UC-Berkeley network station San Andreas Observatory (SAO). The two events are from the 1994 Northridge aftershock sequence and are located within 7 km of each other in the epicenter based on catalog information. Trace 1 (Figure 6a), the reference signal, is from a shallow earthquake (2 km depth), whereas trace 2 (Figure 6b), the primary signal, is from an earthquake occurring at greater depth (12 km). Adaptive filtering to shape the windowed signal from the deeper earthquake to extract the signal common to the shallow event in an attempt to improve subsequent WCC results is applied. A 7s window containing approximately 4.5s of data following the P pick was used. The windowed signal from the deeper event (Figure 6b) was aligned relative to the shallow event signal (Figure 6a) initially by the P picks, and then fine-tuned by applying a lag search. The zero-lag CC between the primary and filtered traces (Figure 6c) and the signal-to-noise ratio of the filtered trace relative to the error trace (Figure 6d) have coincident maxima. After five iterations of the CANC algorithm, the signal from the deeper event is successfully decomposed into an estimate of the common signal (Figure 6e) and the dissimilar error signal (Figure 6f).

We can compare the estimate of common signal to individual trace output by the application of coherency filtering. Shown are the coherency-filtered traces for the shallow and deep event (Figures 6g and h). The frequency content of the two clustered events is very similar. Consequently, coherency filtering yields output traces similar to the original trace data. The adaptive filter shaping of the deep event's waveform visually yields a signal (Figure 6e) closer in appearance to the shallow event (Figure 6a). Application of adaptive filtering increases the maximum CC value for the shallow event with the CANC-filtered trace from 0.51 to 0.83. CC of the coherency-filtered data yields a

maximum value of 0.70. These CC maxima occur at the same lag. Thus the CANC approach can successfully extract a more similar waveform from the primary signal than coherency filtering while preserving timing.

Double-difference multiple-event location and tomography

We have developed the new method of double-difference (DD) tomography. The code tomoDD takes the DD location method (hypoDD) a step further to solve for 3D velocity structure simultaneously with hypocenter locations, using both catalog picks and differential arrival times. Compared to conventional tomography, the result is a sharpening of the seismicity distribution equal in quality to hypoDD plus a sharpening of the velocity image due to removal of the majority of the location scatter. We have developed local- (Zhang and Thurber, 2003a) and regional-scale (Zhang *et al*., 2004) versions of tomoDD, and have applied each to a number of synthetic and real datasets. The local-scale version of the tomoDD code, along with a users manual and sample dataset, is currently available on the web (http://www.geology.wisc.edu/~hjzhang/download.htm). We have also developed a preliminary JHD version of the new location code locOO (Ballard, 2003) as a first step towards the creation of a DD version of the code.

CONCLUSIONS AND RECOMMENDATIONS

Advances in techniques for waveform alignment, event clustering, waveform decomposition, and location and tomography have been achieved with the support of this contract. We echo the conclusion voiced by Prof. Paul Richards that a quantum change is needed in the manner in which earthquake locations are determined in the seismic monitoring environment (both nuclear and otherwise). Effective tools for event clustering, waveform alignment, and joint location/tomography are available, and a concerted effort will be required to implement these tools in "real-world" monitoring situations. Accomplishing this will probably require closer and more direct interaction between the tool developers and the users, in particular to allow for direct feedback from the users to the developers.

ACKNOWLEDGEMENTS

We thank Wayne Du, Bill Lutter, Jean Battaglia, Rick Aster, and Wenzheng Yang for their contributions to this paper, Megan Flanagan for providing the code for the spherical earth finite-difference method, Chris Young and Sandy Ballard for assistance with locOO, and Charlotte Rowe for many valuable discussions.

REFERENCES

Ballard, S. (2003), Seismic event location: dealing with multi-dimensional uncertainty, model non-linearity and local minima, *Proceedings of the 25th Seismic Research Review - Nuclear Explosion Monitoring: Building the Knowledge Base*, 193-202.

Ballard, S. (2003), Seismic event location: dealing with multi-dimensional uncertainty, model non-linearity and local minima, Proceedings of the 25th Seismic Research Review: Building the Knowledge Base (September 23-25, Tucson, Arizona, 2003), 193-202.

Du, W., C. H. Thurber, and D. Eberhart-Phillips (2004), Earthquake relocation using cross-correlation time delay estimates verified with the bispectrum method, *Bull. Seismol. Soc. Am.*, 94, 856-866.

Hattingh, M. (1988), A new data adaptive filtering program to remove noise from geophysical time- or space-series data, *Comp. Geosci.*, 14, , 467-480.

Nikias, C. L. *and* R. Pan (1988), Time delay estimation in unknown Gaussian spatially correlated noise, *IEEE Trans. Acoust. Speech Signal Processing*, 36, 1706-1714.

Nikias, C. L. *and* M. R. Raghuveer (1987), Bispectrum estimation: A digital signal processing framework, *Proc. IEEE*, 75, 869-891.

Poupinet, G., W. L. Ellsworth, and J. Fréchet (1984), Monitoring velocity variations in the crust using earthquake doublets: an application to the Calaveras fault, California, *J. Geophys. Res.*, 89, 5719-5731.

Rowe, C. A., R.C. Aster, B. Borchers and C. J. Young (2002), An automatic, adaptive algorithm for refining phase picks in large seismic data sets, *Bull. Seismol. Soc. Amer*, 92, 1660-1674.

Rubin, A., D. Gillard, and J. Got (1999), Streaks of microearthquakes along creeping faults, *Nature*, 400, 635-641.

Schaff, D. P., G. H. R. Bokelmann, G. C. Beroza, F. Waldhauser, and W. L. Ellsworth (2002), High-resolution image of Calaveras Fault seismicity, *J. Geophys. Res.*, 107, 2186, doi:10.1029/2001JB000633.

Shearer, P. M. (1997), Improving local earthquake locations using the L1 norm and waveform cross correlation: Application to the Whittier Narrows, California, aftershock sequence, *J. Geophys. Res.*, 102, 8269-8283.

Ulrych, T. J., M. D. Sacchi, and J. M. Graul (1999), Signal and noise separation: art and science, *Geophys.*, 64, 1648-1656.

Waldhauser, F. and W.L. Ellsworth (2000), A double-difference earthquake location algorithm: Method and application to the Northern Hayward Fault, California, *Bull. Seism. Soc. Am.*, 90, 1353-1368.

Young, C. J., E. P. Chael, and B. J. Merchant (2002), Version 1.7 of MatSeis and the GNEM R&E regional seismic analysis tools, *Proc. 24th Seismic Research Review*, 915-924.

Zhang, H. *and* C. H. Thurber (2003), Double-difference tomography: The method and its application to the Hayward fault, California, *Bull. Seism. Soc. Am.*, 93, 1875-1889.

Zhang, H., C. H. Thurber, C. A. Rowe (2003), Automatic first-arrival detection and picking with multiscale wavelet analysis, *Bull. Seism. Soc. Am*., 93(5), 1904-1912.

Zhang, H., C. Thurber, D. Shelly, S. Ide, G. Beroza, and A. Hasegawa (2004), High-resolution subducting slab structure beneath N. Honshu, Japan, revealed by double-difference tomography, *Geology*, 32, 361-364.

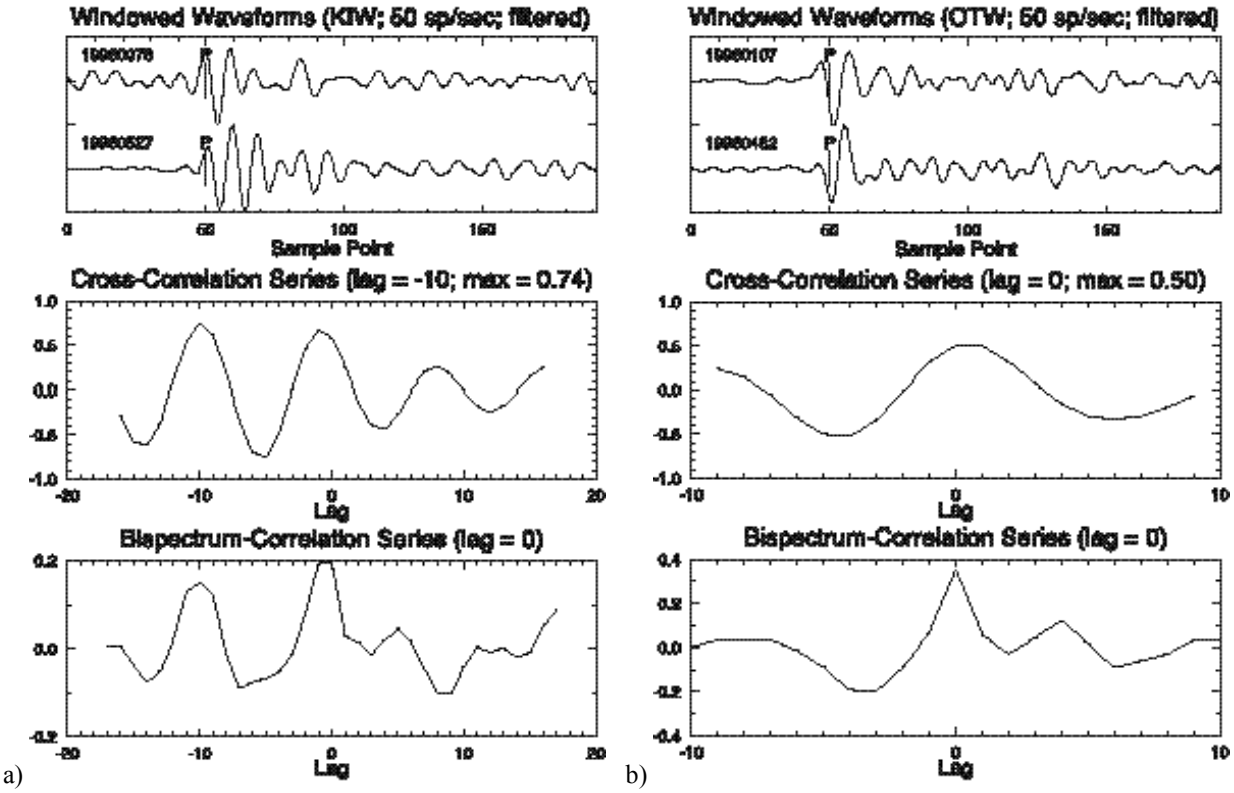

a) b)

Figure 1. Examples of a) rejection of a high CC value due to inconsistent results between the CC and BS lags and b) acceptance of a low CC value due to consistent results between the CC and BS lags.

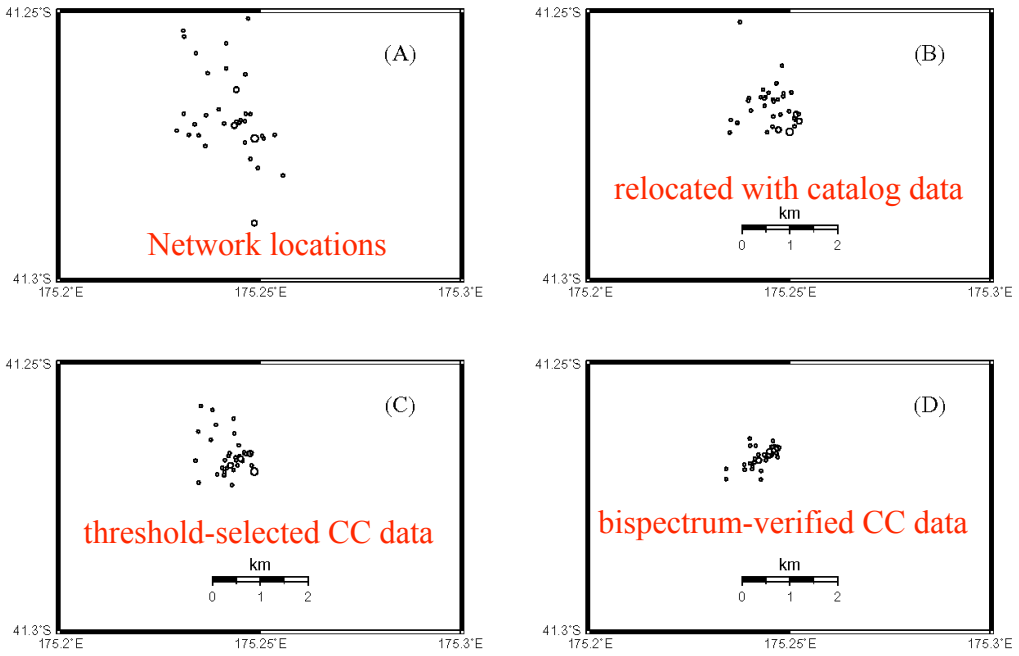

Figure 2. Example of successive improvement in location clustering of a set of earthquakes in New Zealand, comparing catalog locations to those obtained by use of DD location with catalog picks, then with threshold-selected CC data, and finally with BS-verified CC data.

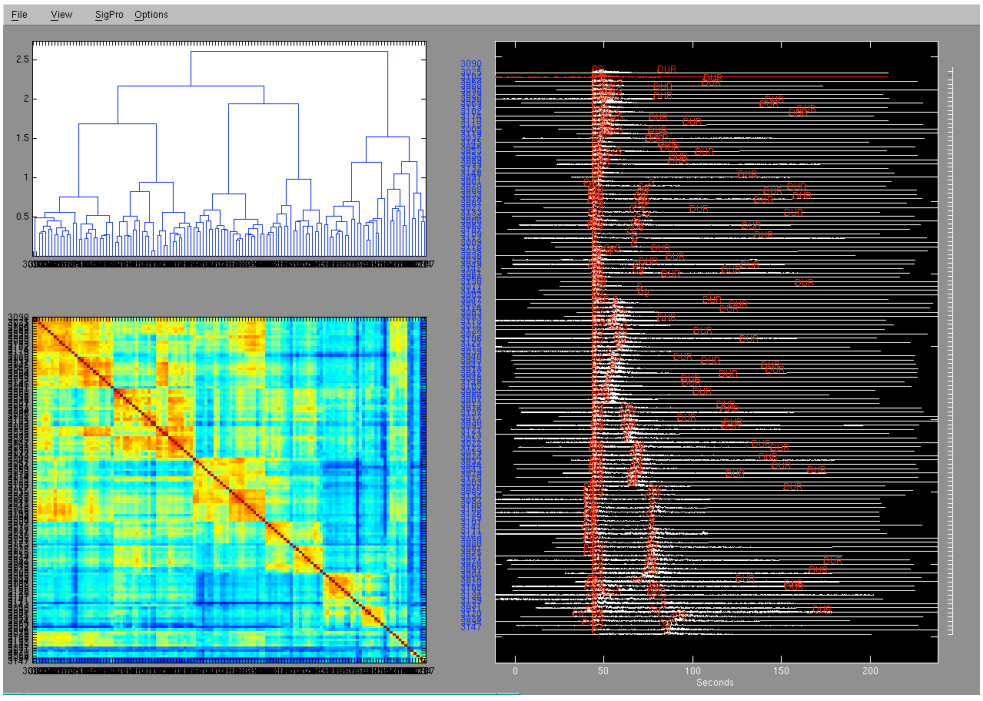

Figure 3. Reference waveforms for station CAR are shown at right, also showing the cross-correlation coefficient matrix of each waveform pair (left, bottom) and corresponding dendrogram (left, top).

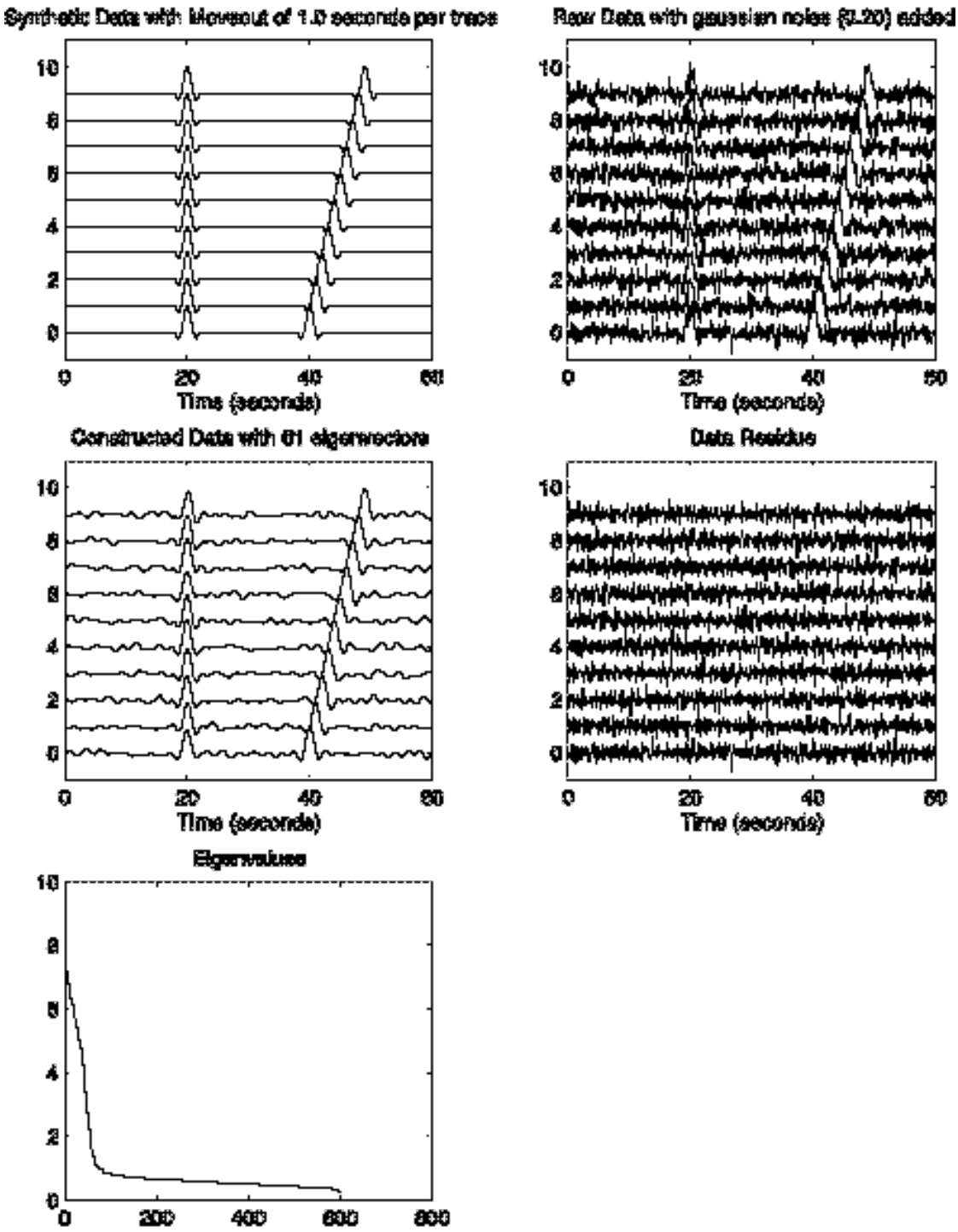

Figure 4. Example application of KLD to a set of seismograms with a pair of "arrivals" only one of which is time-aligned across the records (top left), with noise added (top right). The data reconstructed from the 61 eigenvectors with eigenvalues above average in size (bottom left) retains both the time-aligned arrival and the arrival with moveout (middle left), leaving little signal energy in the residual image (middle right). In contrast, eigenimage decomposition cannot reconstruct both arrivals adequately.

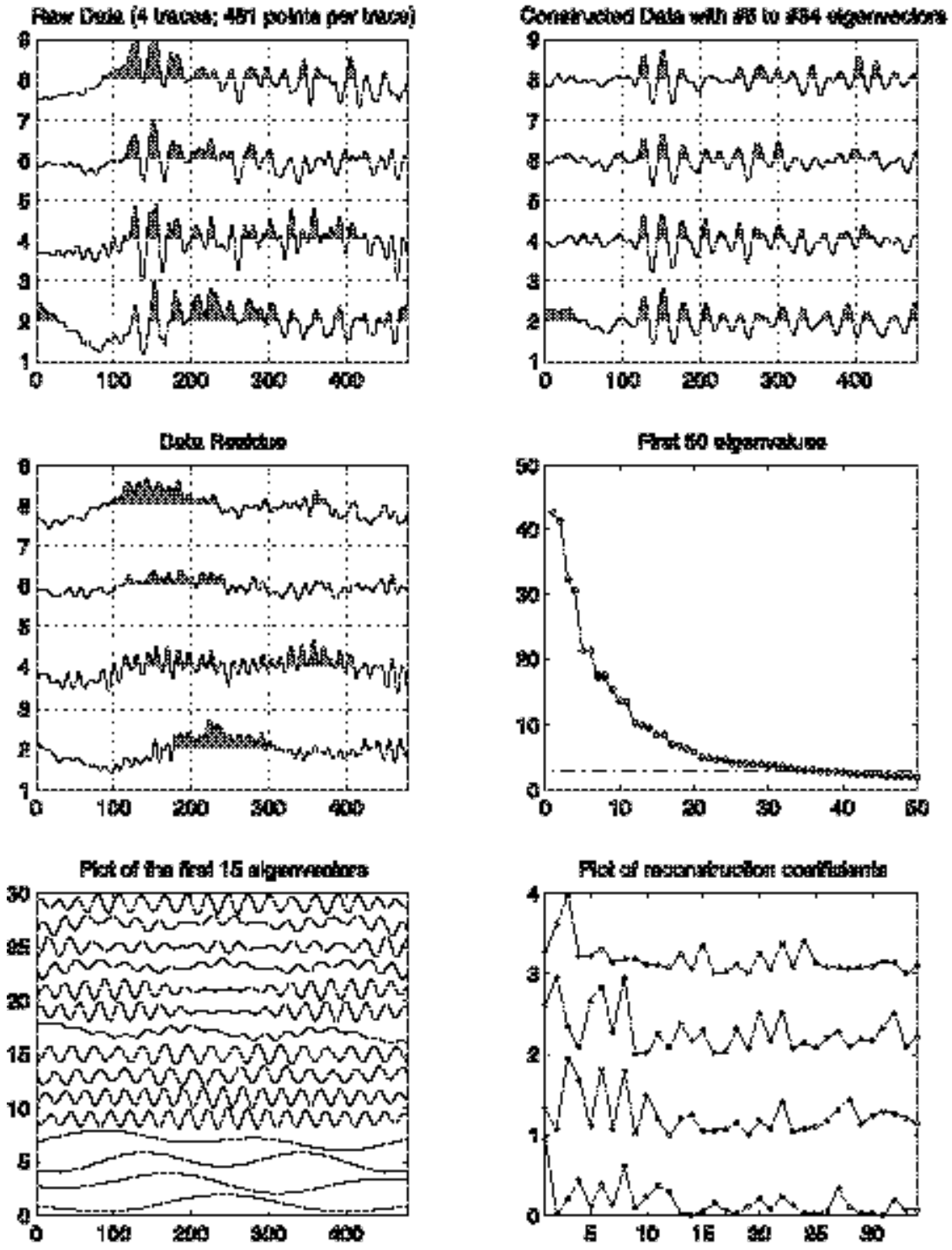

Figure 5. Example application of KLD to real data (upper left). Large and small eigenvalues were excluded in this case. The reconstructed data (upper right) from the 30 eigenvectors with eigenvalues from #5 to #34 (middle right) produces similar looking waveforms, leaving relatively little energy in the residual image (middle left). The eigenvectors for the larger eigenvalues (lower left) and their corresponding reconstructions (lower right) show the long-period noise character of the first 4 eigenvectors.

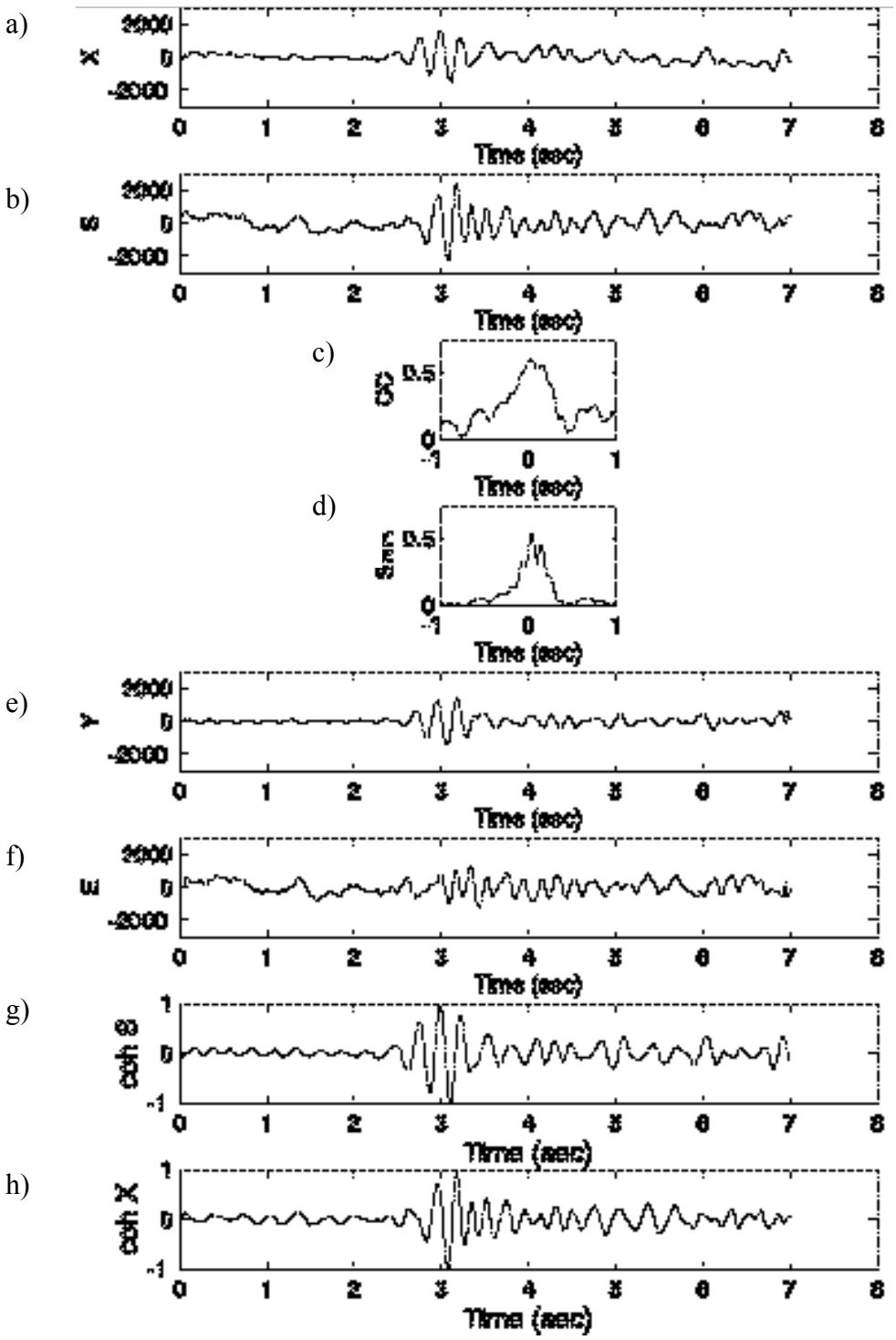

Figure 6. a,b) Seismic data windowed around the P arrival for the a) shallow (2 km) and deep (12 km) earthquakes from Northridge (S. California) cluster. The shallow event is used as the reference signal and the deeper event is used as the primary signal; noise has been added to the latter trace. c) Zero-lag cross-correlation between the primary and CANC-filtered traces for a range of signal alignments (see text). d) SNR for the CANC-filtered trace versus the error trace for a range of signal alignments. e) Common signal obtained from CANC adaptive filter. f) Error trace. Coherency filtering applied to data in a) and b) results in the signal traces displayed in g) and h), respectively.